Low-lying electronic states of InBi: A configuration interaction study

ARTICLE *in* JOURNAL OF MOLECULAR STRUCTURE THEOCHEM · MAY 2003

Impact Factor: 1.37 · DOI: 10.1016/S0166-1280(03)00007-1

3 AUTHORS, INCLUDING:

Surya Chattopadhyaya
Tripura University
16 PUBLICATIONS **61** CITATIONS

SEE PROFILE

ELSEVIER

Journal of Molecular Structure (Theochem) 625 (2003) 95–109

THEO CHEM

www.elsevier.com/locate/theochem

Low-lying electronic states of InBi: a configuration interaction study

Anjan Chattopadhyay, Surya Chattopadhyaya, Kalyan Kumar Das*

Department of Chemistry, Physical Chemistry Section, Jadavpur University, Kolkata 700 032, India

Received 14 August 2002; accepted 16 December 2002

Abstract

Multireference singles and doubles configuration interaction (MRDCI) method has been used to study the low-lying electronic states of InBi. The calculations include relativistic effective core potentials (RECP) and spin–orbit operators of In and Bi atoms. Potential energy curves of 46 Λ–S states, of which 34 states correlate with the lowest three dissociation limits, have been computed. Spectroscopic properties of 22 Λ–S bound states of InBi within 42,000 cm^{-1} of energy are reported. The dissociation energy of the ground state of InBi is estimated to be 114 kJ mol^{-1} as compared with the observed value of 153.6 ± 1.7 kJ mol^{-1}. The influence of d-correlation on the ground state has been tested. Effects of the spin–orbit coupling on the potential energy curves and spectroscopic parameters are studied. Transition probabilities of electric dipole-allowed transitions such as $A^3\Pi-X^3\Sigma^-$, $A^3\Pi-{}^3\Pi$, $2^1\Sigma^+-{}^1\Pi$, $2^1\Sigma^+-{}^1\Sigma^+$ are calculated. The radiative lifetimes of $A^3\Pi$ and $2^1\Sigma^+$ at $v' = 0$ are found to be 1.0 and 7.2 μs, respectively. The $A0^+$ state is identified as an important state which survives from the predissociation. Three transitions such as $A0^+-X_10^+$, $A0^+-X_21$, and $A0^+-{}^3\Pi_{0^+}$ are studied. The MRDCI estimated spectroscopic properties of InX (X = P, As, Sb, Bi) molecules are compared.

Keywords: Electronic states; Spin–orbit coupling; Potential energy curves

1. Introduction

The compounds of group III and V, and their neutral and ionic clusters have drawn a considerable attention in the past few decades [1–40] due to the semiconducting properties. Besides their importance as materials for preparing electronic devices, the electronic structure and spectroscopic aspects of the molecules themselves have been explored experimentally as well as theoretically. The pioneering work on the clusters of gallium arsenide has been carried out by Smalley and co-workers [1–6]. These authors have used laser induced photoionization and the time-of-flight mass spectrometry measurement techniques for this purpose. The resonant two-photon ionization spectroscopy for the electronic structure and spectroscopic properties of the jet-cooled GaAs molecule have been carried out by Lemire et al. [7]. The negative ion zero-electron kinetic photodetachment spectroscopic techniques to study the electronic states of the neutral group IV and group III–V clusters have been attempted in recent years [8–12].

* Corresponding author. Fax: +91-33-473-1484.
E-mail addresses: das_kalyank@yahoo.com (K.K. Das), kalyankd@hotmail.com (K.K. Das), kalyankd@vsnl.net (K.K. Das).

0166-1280/03/$ - see front matter © 2003 Elsevier Science B.V. All rights reserved.
doi:10.1016/S0166-1280(03)00007-1

The matrix-isolated electron-spin-resonance (ESR) spectra of small clusters of Ga, Si, Sn, and mixed group III–V elements have been recorded by Weltner and co-workers [13–16]. The infrared absorption spectra of GaX and InX (X = P, As, Sb) molecules in rare-gas matrices have also been observed by laser vaporization techniques [13–15]. Piacente and Desideri [17] have investigated mass-spectra to determine the gas-phase dissociation energy of the GaBi molecule. The isovalent molecules such as TlAs and TlBi have been also studied from the similar investigations. Unlike the lighter group III–V compounds, which are semiconductors at ambient conditions, the heavier molecule like InBi forms a semimetallic compound with tetrahedral structure. The gas-phase dissociation energy of the InBi molecule at 298 K has been reported [18] to be 153.6 ± 1.7 kJ mol^{-1}. So far, no attempts have been made to study theoretically or experimentally the electronic structure and spectroscopic properties of the InBi molecule in gas-phase or in matrix.

Theoretical studies of the spectroscopic properties and electronic structure of molecules of group III and V are made possible in recent years because of the advancement of the computer technology and the availability of theoretical methods. In this context the review articles of Balasubramanian [19,20] relating the relativistic effects on molecules and clusters are important to mention. The complete active space self-consistent field (CASSCF) configuration interaction (CI) calculations at different levels including relativistic effects have been performed by Balasubramanian and co-workers [21–29] on di and triatomic molecules and ions of group III and V. Large scale CI calculations on the low-lying electronic states of a lighter molecule such as AlP have been carried out by Meier et al. [30]. The local spin density method has been used by Russo and co-workers [31–33] to study the electronic states of CuIn, AgIn, CuGa, AgGa, etc. and their clusters. Recently systematic studies on the low-lying electronic states of diatomic molecules of group III and V have been made by Das and co-workers [34–40] using ab initio based multi-reference singles and doubles configuration interaction (MRDCI) calculations. Each of these molecules shows the presence of $A^3\Pi$–$X^3\Sigma^-$ bands which are sufficiently strong to be observed. However, the A–X band of GaAs has been observed only in the gas-phase. It is experimentally known that three components of $A^3\Pi$ of GaAs, namely, $A^3\Pi_{2,1,0^-}$ undergo predissociation, while the $A^3\Pi_{0^+}$ component survives. The MRDCI studies agree well with these result, and it also predicts similar situation for the isovalent molecules. A comparative study of the computed properties of GaP, GaAs, GaSb, and GaBi molecules at the same level of CI calculations has also been carried out very recently [40].

The present paper is intended, for the first time, to study theoretically, the electronic spectrum of the InBi molecule. Potential energy curves and spectroscopic parameters of low-lying electronic states are computed by using MRDCI method which takes care of the relativistic effect through pseudopotentials. The spin–orbit coupling, which becomes important for such a heavy molecule like InBi, is also included in the calculations. Transition probabilities of dipole allowed transitions including those, which are spin-forbidden, are estimated. Similar with other diatomic molecules of group III–V, the A–X transition is studied here with a special attention. The radiative lifetimes of the upper states at the lower vibrational levels are also the subject of the present study.

2. Details of the computational treatment

The CI calculations of heavy molecules with many electrons are made possible because of the availability of effective core potentials of atoms. The $4d^{10}5s^25p^1$ electrons of In and $5d^{10}6s^26p^3$ electrons of Bi are retained in the valence space, while the inner electrons of both atoms are replaced by the semicore type relativistic effective core potentials (RECP) of the corresponding atom. RECP of LaJohn et al. [41] are used for the In atom, while pseudo potentials of the bismuth atom are taken from Wildman et al. [42]. The total number of active electrons in the subsequent calculations of InBi is, therefore, reduced to 28. The Cartesian Gaussian basis functions, which are compatible with the above-mentioned RECP, are used without any contraction. Moreover, the optimized 3s3p4d basis set of LaJohn et al. [41] for In is augmented with a set of diffused s and p functions of exponents 0.02 and 0.0145 a_0^{-2}, respectively, taken from Balasubramanian's work [24]. Therefore, the final basis set of In becomes 4s4p4d, while the 6s6p6d

basis set of Bi as suggested by Wildman et al. [42], is used unchanged in this calculation.

A set of self-consistent field (SCF) molecular orbital (MO) calculations for the $\cdots\pi^2\,{}^3\Sigma^-$ state with 28 valence electrons is carried out at each internuclear distance of InBi. The molecule is placed along the $+z$ axis with In at the origin, and the entire calculations have been performed in the C_{2v} subgroup of the actual $C_{\infty v}$ group in which the molecule belongs. The optimized symmetry adapted 100 SCF-MOs are used as basis functions for the CI calculations. Analyzing the MOs at each bond distance, it is seen that all 20 d electrons of In and Bi remain localized on to the respective atoms. These d electrons are, therefore, kept frozen in the CI step. As a result, only eight electrons are to be treated for excitations in CI. The MRDCI codes of Buenker and co-workers [43–49] are used in the present calculations. The low-lying Λ–S states of InBi are computed in the first step without including any spin–orbit coupling. A set of reference configurations is chosen for each irreducible representation in a given spin multiplicity. The CI space is constructed after allowing all single and double excitations from these reference configurations. The size of the largest generated CI space exceeds 5 million. However, the size is reduced below 50,000 by using the configuration selection procedure of Buenker and co-workers [43,44] with a configuration-selection threshold of 2.0 μhartree. The sum of the squares of coefficients of the reference configurations for each root is ≥ 0.93. The energy extrapolation technique along with Davidson's correction [50,51] provides an accurate estimate of the full CI energy. The lowest eight roots are optimized in CI for singlets and triplets, while for quintets only five roots are studied. The entire calculations have been carried out at several bond distances between 3.5 and 18.0 a_0 with different increments ranging 0.05–2.0 a_0. The estimated CI energies and wave functions are then used to determine one electron properties of the low-lying states of the molecule.

The spin–orbit operators for In and Bi atoms, derived from the corresponding RECP, are used to include the spin–orbit coupling in the calculation. The Λ–S CI wave functions are used as basis functions for the spin–orbit calculations in the C_{2v}^2 representation. In the diagonals of the Hamiltonian matrix, the full CI energies are placed, while the spin–orbit coupling elements, which are obtained from the pairs of selected CI wave functions by using spin-projection techniques and Wigner–Eckert theorem, occupy the off-diagonal blocks. In the spin–orbit CI treatment, all 22 Λ–S states correlating with the lowest two dissociation limits are included. Such a two-step method for the inclusion of the spin–orbit interaction has become useful to analyze the Ω-components in terms of different Λ–S eigenfunctions. However, the disadvantage of this simpler two-step method to introduce the spin–orbit coupling is that the spin–orbit is not treated at the same level as the nonrelativistic terms. The resulting eigenvalues and eigenfunctions are then used for estimating spectroscopic constants and transition properties of low-lying Ω states.

The nuclear Schrödinger equations are solved numerically [52] after fitting the potential energies of both Λ–S and Ω states of the molecule into polynomials. Transition dipole moments involved in a particular transition, are computed for the pair of vibrational functions. Subsequently, spontaneous emission coefficients and hence transition probabilities are calculated. Finally, radiative lifetimes (partial or total) of excited states at different vibrational levels are estimated from the respective transition probability data.

3. Results and discussion

3.1. Potential energy curves and spectroscopic properties of Λ–S states

The ground state ($5s^25p$; ^2P_u) of the Indium atom combines with the high-spin ground state ($6s^26p^3$; ^4S_u) of Bi to generate four molecular states of triplet and quintet spin multiplicities, namely, $^3\Sigma^-$, $^3\Pi$, $^5\Sigma^-$, and $^5\Pi$. The observed atomic energy levels show that the next two excited states of In contain a Rydberg function (6s) and are lying well above the ground state. On the other hand, the first excited state ($6s^26p^3$; ^2D_u) of Bi is low-lying and interacts with the ground-state indium atom to correlate with 18 low-lying Λ–S states, namely, Σ^+, $\Sigma^-(2)$, $\Pi(3)$, $\Delta(2)$, and Φ of singlet and triplet spin multiplicities. In the absence of the spin–orbit coupling, the observed j-averaged relative energy of the second dissociation

limit $In(^2P_u) + Bi(^2D_u)$ is above the MRDCI estimated value by about 2200 cm^{-1}. Six singlets and six triplets of $\Sigma^+(2)$, Σ^-, $\Pi(2)$, and Δ symmetries correlate with the $In(^2P_u) + Bi(^2P_u)$ asymptote. In Fig. 1a and b, we have plotted the computed potential energy curves of 34 quintet, triplet, and singlet Λ–S states which correlate with the lowest three asymptotes. Besides, curves of some of the high-lying electronic states, mainly quintets, are also plotted in the Franck–Condon region. There are 19 Λ–S states, which are bound within 42,000 cm^{-1} of energy. The remaining states are mostly repulsive in nature. Spectroscopic constants (T_e, r_e, ω_e) of these bound states, estimated by fitting the potential curves, are summarized in Table 1. The ground state ($X^3\Sigma^-$) of InBi is represented mainly by an open shell configuration $\sigma^2\sigma^{*2}\sigma'^2\pi^2$, which is analogous with other isovalent molecules of group III and V elements. The bond length and vibrational frequency of the ground-state InBi molecule at the potential minimum are 3.01 Å and 120 cm^{-1}, respectively. No experimental or theoretical results of InBi are available for comparison. However, the MRDCI treatment used here tends to result a somewhat larger r_e and smaller ω_e. In the potential minimum of the ground state, the σ MO is mostly nonbonding s atomic orbital localized on Bi. The next important orbital (σ^*) comprises s(In) and s, p_z(Bi) atomic orbitals with antibonding combinations. On the other hand, the σ' orbital is found to be strongly bonding with respect to s and p_z atomic orbitals of both In and Bi. In the Franck–Condon region, the π MO is mostly pure nonbonding $p_{x,y}$ atomic orbitals, which are localized on Bi. However, a very weak bonding characteristic with $p_{x,y}$(In) has been noted in π MO at some bond distances. The next π^* MO is strongly antibonding combination of $p_{x,y}$ atomic orbitals of In and Bi. The computed ground-state dissociation energy (D_e) of InBi from the MRDCI treatment at a very long bond distance, is found to be 114 kJ mol^{-1}, which is an underestimation of the experimental value by about 39 kJ mol^{-1}. Some improvement is expected after the inclusion of 20 d-electrons in the CI step and the enhancement of the basis sets. Earlier calculations on isovalent molecules have shown that the calculated D_e value is always smaller than the observed one by

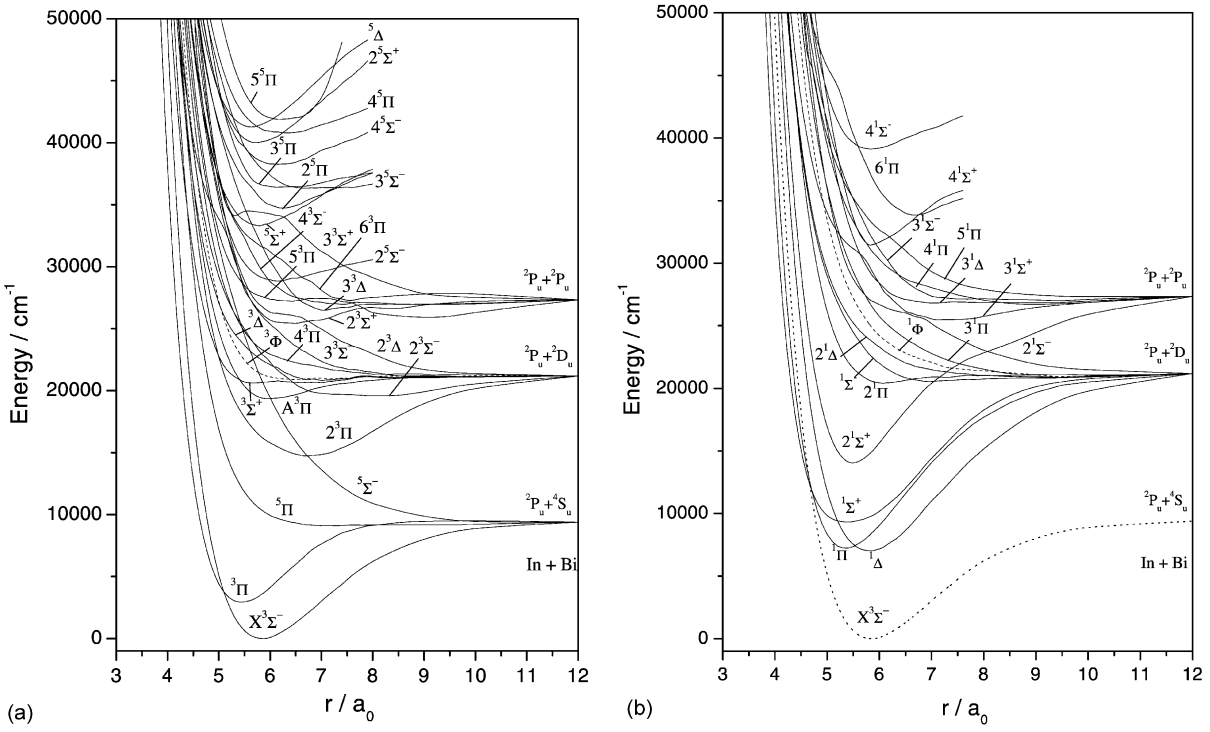

Fig. 1. (a) Potential energy curves of triplet and quintet Λ–S states of InBi. (b) Potential energy curves of singlet Λ–S states of InBi.

Table 1
Spectroscopic parameters of low-lying Λ–S States of InBi

State	T_e (cm^{-1})	r_e (Å)	ω_e (cm^{-1})
$X^3\Sigma^-$	0	3.10	120
$^3\Pi$	2893	2.88	138
$^1\Delta$	6981	3.07	127
$^1\Pi$	7183	2.85	151
$^1\Sigma^+$	9105	2.85	117
$2^1\Sigma^+$	14,080	2.91	165
$2^3\Pi$	14,776	3.56	73
$A^3\Pi$	19,365	3.18	88
$2^1\Pi$	20,420	3.22	84
$^3\Sigma^+$	20,615	3.00	87
$2^3\Sigma^+$	25,406	3.39	74
$3^1\Sigma^+$	25,480	3.82	54
$2^5\Sigma^-$	28,874	3.27	81
$4^1\Sigma^+$	31,249	2.99	118
$^5\Sigma^+$	33,358	3.06	108
$2^5\Pi$	34,801	3.32	93
$4^5\Sigma^-$	38,206	3.24	95
$4^1\Sigma^-$	39,132	3.10	102
$2^5\Sigma^+$	39,990	3.05	122
$4^5\Pi$	40,755	3.31	76
$^5\Delta$	41,258	2.99	125
$5^5\Pi$	41,821	3.28	95

0.3–0.6 eV because of the use of the effective core potential approximation. The CI calculations for the ground state have been repeated by allowing 20 frozen d electrons to participate in the active space. The ground-state dissociation energy becomes 109 kJ mol^{-1} as compared with the value of 114 kJ mol^{-1} without d-correlations. However, the bond length (r_e) is shortened by about 0.04 Å, while ω_e is increased only by 7 cm^{-1}.

In general, two singlet states of $^1\Sigma^+$ and $^1\Delta$ symmetries are generated from the ground-state electronic configuration ($\cdots\pi^2$). As seen in Table 1, the $^1\Delta$ state of InBi lies 6981 cm^{-1} above the ground state with $\omega_e = 127$ cm^{-1}. The computed r_e of the $^1\Delta$ state is comparable with that of the ground state. The composition of the $^1\Sigma^+$ state is found to be complicated. Analyzing the CI wave functions of $^1\Sigma^+$ in the Franck–Condon region, it has been found that a closed-shell configuration $\cdots\sigma^2\sigma^{*2}\pi^4$ interacts strongly with the open shell one such as $\cdots\sigma^2\sigma^{*2}\sigma'^2\pi^2$. A strong avoided crossing between the potential curves of $^1\Sigma^+$ and $2^1\Sigma^+$ states makes the minimum of $^1\Sigma^+$ shallow. As a result, the potential minimum of the $2^1\Sigma^+$ state becomes comparatively narrow. Although it is not clear from Fig. 1b, the analysis of CI wave functions at different bond distances before and after 5.5 a_0 confirms the avoided crossing of the curves of two states of the $^1\Sigma^+$ symmetry. The r_e and ω_e of the $^1\Sigma^+$ state, obtained from the adiabatic curve, are 2.85 Å and 117 cm^{-1}, respectively, while the corresponding values of the excited $2^1\Sigma^+$ state are 2.91 Å and 165 cm^{-1}. At equilibrium, the estimated transition energy of $^1\Sigma^+$ is 9105 cm^{-1}, while the energy gap between $^1\Sigma^+$ and $2^1\Sigma^+$ states is nearly 5000 cm^{-1}. Three states, namely, $X^3\Sigma^-$, $^1\Sigma^+$, and $2^1\Sigma^+$ dissociate into three successive asymptotes.

Similar with other isovalent molecules, the first excited state of InBi is of the $^3\Pi$ symmetry. The state is lying only 2893 cm^{-1} above the ground state and is reasonably strongly bound. The $^3\Pi$ state is mainly generated from the single excitation of the type $\sigma' \rightarrow \pi$. However, another configuration arising out of the $\sigma' \rightarrow \pi^*$ excitation also contributes significantly to the $^3\Pi$ state. The singlet counterpart of $^3\Pi$ originates from the same excitations. The computed energy gap between $^3\Pi$ and $^1\Pi$ states of InBi is about 4290 cm^{-1}. Analogous with other isovalent molecules of group III and V, the In–Bi bond in the $^3\Pi$ state is at least 0.22 Å shorter than the ground-state bond. The $^1\Pi$ state is found to have even shorter r_e and larger ω_e as compared with its triplet counterpart. The $^3\Pi$ state correlates with the lowest asymptote, while the $^1\Pi$ state dissociates into $In(^2P_u) + Bi(^2D_u)$. In general, the larger stability of the bond in the $^{1,3}\Pi$ states is quite common for these types of molecules, and it is mainly due to the increase in the delocalization of π MOs.

The $\sigma' \rightarrow \pi^*$ excitation generates four $^3\Pi$ states, of which $2^3\Pi$ and $3^3\Pi$ states are bound, while $4^3\Pi$ and $5^3\Pi$ are repulsive. The situation is very similar with other group III–V diatomic molecules. The potential minimum of the $2^3\Pi$ state with $T_e = 14,776$ cm^{-1} appears at a longer bond distance ($r_e = 3.56$ Å). However, the compositions of CI wave functions at different bond lengths have shown a strong avoided crossing between two curves of the $^3\Pi$ symmetry with $\cdots\sigma'\pi^2\pi^*$ and $\cdots\sigma'\pi^3$, respectively, as the dominant configuration. The broad minimum of the $2^3\Pi$ state is thus only due to such a curve crossing. The vibrational frequency (ω_e) of the $2^3\Pi$ state is only 73 cm^{-1}. Earlier MRDCI calculations of isovalent molecules have revealed

the identical pattern of the $2^3\Pi$ state. The $2^3\Pi$–$X^3\Sigma^-$ transition is expected to be very weak because of a very small Franck–Condon factor. The $3^3\Pi$ state is denoted as $A^3\Pi$, which is analogous with the observed A state of GaAs. The computed transition energy of the $A^3\Pi$ state at the potential minimum is about 19,365 cm^{-1}. The estimated r_e and ω_e values of this state are 3.18 Å and 88 cm^{-1}, respectively. However, the $A^3\Pi$ state is weakly bound, and the calculated binding energy is only 0.22 eV. There remains a scope to compare the spectroscopic properties of $A^3\Pi$ for the isovalent molecules like InP, InAs, InSb, and InBi. The CI wave functions show that the $A^3\Pi$ state is almost purely represented by the $\cdots\sigma'\pi^2\pi^*$ configuration. As seen in Fig. 1a, $2^3\Pi$, $A^3\Pi$, and $4^3\Pi$ states dissociate into the $In(^2P_u) + Bi(^2D_u)$ limit. The spin–orbit components of the $A^3\Pi$ state play an important role in determining the spin–orbit effect on the A–X band. Both $5^3\Pi$ and $6^3\Pi$ states, which correlate with the $In(^2P_u) + Bi(^2P_u)$ limit, are repulsive.

The $2^1\Pi$ state of InBi comes next to $A^3\Pi$ in energy. It is, however, very weakly bound (binding energy $\sim$ 600–700 cm^{-1}) with $T_e = 20,420$ cm^{-1} and $r_e = 3.22$ Å. Comparing the electronic spectrum of four InX (X = P, As, Sb, Bi) molecules, the binding energy of the $2^1\Pi$ state decreases with the increase in the mass of the molecule. The present calculations suggest that the $\cdots\sigma'\pi^2\pi^*$ configuration dominates in the $2^1\Pi$ state along with other two open shell configurations. In total, 10 Λ–S states originate from the $\cdots\sigma'\pi^2\pi^*$ configuration. Four states of the $^3\Pi$ symmetry are already mentioned. Except $2^1\Pi$, two other singlet Π states, namely, $3^1\Pi$ and $4^1\Pi$ are repulsive in nature. The remaining three states such as $^1\Phi$, $^3\Phi$, and $^5\Pi$, which are represented by the same $\cdots\sigma'\pi^2\pi^*$ configuration, are also repulsive. As seen in Fig. 1a–b, the $^5\Pi$ state dissociates into the lowest asymptote, while $^{1,3}\Phi$ states correlate with the second limit.

The $^3\Sigma^+$ state, which is obtained from a single excitation such as $\cdots\pi^4 \rightarrow \cdots\pi^3\pi^*$, has a very shallow potential minimum ($\omega_e = 87$ cm^{-1}) around $r = 3.0$ Å with only one vibrational node. For other InX (X = P, As, Sb) molecules, this state has been found to be relatively strongly bound. Other states originating from the $\cdots\pi^3\pi^*$ configuration are found to be mostly repulsive. The $2^3\Sigma^+$ state, whose potential minimum is lying 5000 cm^{-1} above $^3\Sigma^+$, is also weakly bound. The compositions of CI wave functions of $^3\Sigma^+$ and $2^3\Sigma^+$ reveal that in the longer bond length region of the potential energy curve of $2^3\Sigma^+$, two important configurations, namely, $\cdots\pi^3\pi^*$ and $\cdots\sigma'^2\pi\pi^*$ mix up strongly. Even at the potential minimum ($r_e = 3.39$ Å), the $2^3\Sigma^+$ state is an admixture of $\cdots\sigma'^2\pi\pi^*$ ($c^2 = 0.53$) and $\cdots\pi^3\pi^*$ ($c^2 = 0.26$). A maximum also appears in the curve of $3^3\Sigma^+$ around $r = 6.0$ a_0 due to an avoided crossing with a repulsive curve of the same symmetry dominated by the $\cdots\sigma\sigma'\pi^2$ configuration.

Fig. 1b shows a sharp avoided crossing between the potential curves of $3^1\Sigma^+$ and $4^1\Sigma^+$ in the range $r = 5.5$–5.8 a_0. The low-lying shallow minimum ($r_e = 3.82$ Å) corresponds to the $3^1\Sigma^+$ state which is represented predominantly by the $\cdots\sigma'^2\pi\pi^*$ configuration. The spectroscopic constants are estimated from the diabatic curve of the $4^1\Sigma^+$ state which is a mixture of several configurations. A number of quintet states exists in the electronic spectrum of InBi within 42,000 cm^{-1}. The $^5\Sigma^-$ state, which dissociates into the lowest limit, is repulsive. However, the $2^5\Sigma^-$ state

Table 2
Dissociation relation between Ω states and atomic states of InBi

Ω state	Atomic states, In + Bi	Relative energy (cm^{-1})	
		Expt.[a]	Calc.
0^+, 0^-, 1(2), 2	$^2P_{1/2} + {}^4S_{3/2}$	0	0
$0^+(2)$, $0^-(2)$, 1(3), 2(2), 3	$^2P_{3/2} + {}^4S_{3/2}$	2213	2016
0^+, 0^-, 1(2), 2	$^2P_{1/2} + {}^2D_{3/2}$	11,419	12,346
$0^+(2)$, $0^-(2)$, 1(3), 2(2), 3	$^2P_{3/2} + {}^2D_{3/2}$	13,632	14,324
0^+, 0^-, 1(2), 2(2), 3	$^2P_{1/2} + {}^2D_{5/2}$	15,438	17,055
$0^+(2)$, $0^-(2)$, 1(4), 2(3), 3(2), 4	$^2P_{3/2} + {}^2D_{5/2}$	17,650	19,075

[a] Ref. [53].

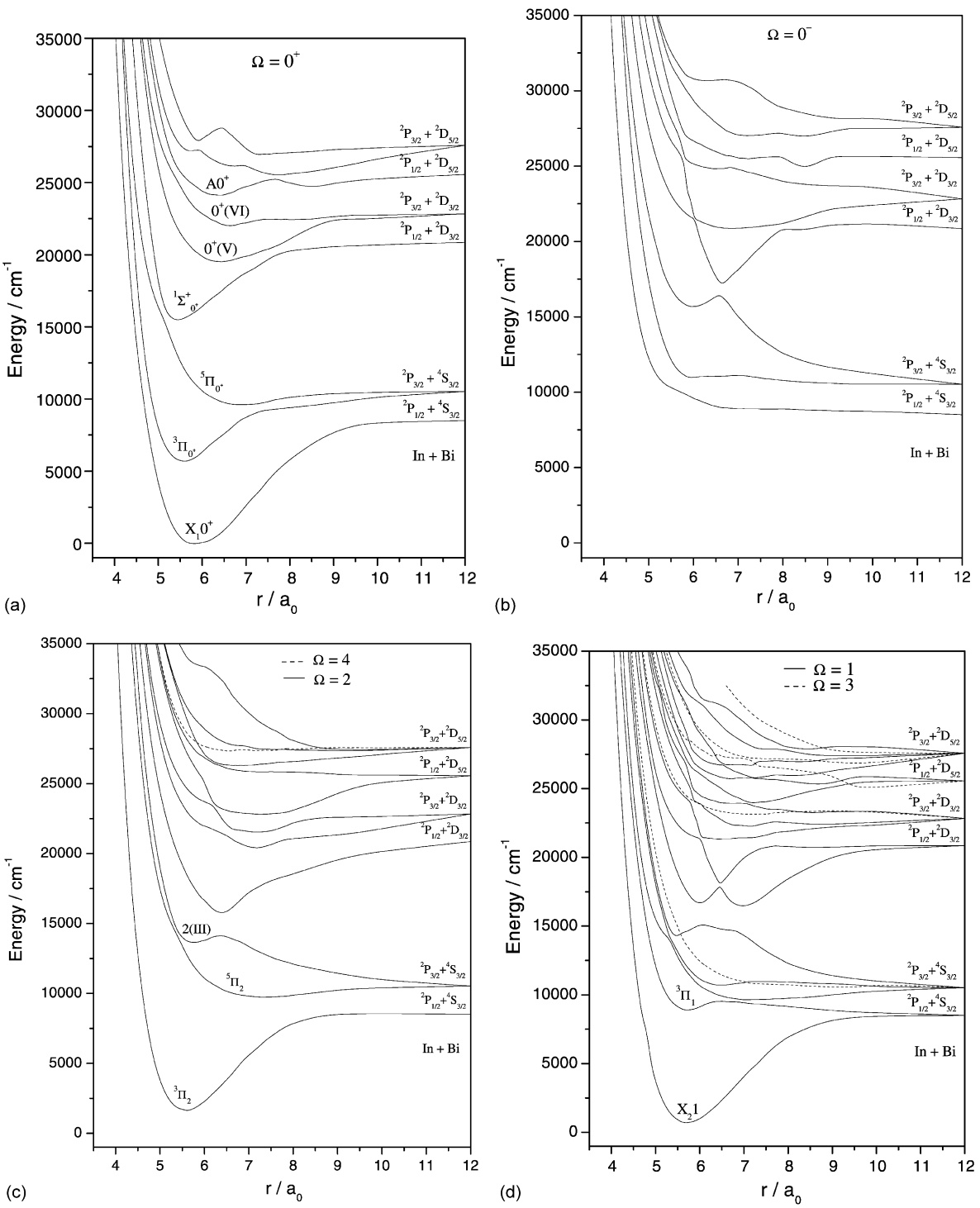

Fig. 2. (a) Potential energy curves of the low-lying $\Omega = 0^+$ states of InBi. (b) Potential energy curves of the low-lying $\Omega = 0^-$ states of InBi. (c) Potential energy curves of the low-lying $\Omega = 2$ and 4 states of InBi. (d) Potential energy curves of the low-lying $\Omega = 1$ and 3 states of InBi.

is weakly bound at the longer bond length region ($r_e = 3.27$ Å) with an estimated transition energy of 28,874 cm^{-1}. The state is described mainly by $\cdots\sigma'\sigma_5\pi^2$, where σ_5 MO has some Rydberg character of the 7s atomic orbital of Bi. The basis set used in this calculation needs additional Rydberg functions for the better description of the $2^5\Sigma^-$ state. The lowest state of the $^5\Sigma^+$ symmetry is lying 33,358 cm^{-1} above the ground state with $r_e = 3.06$ Å and $\omega_e = 108\ cm^{-1}$. Three important configurations, such as $\cdots\pi^2\pi^{*2}$ ($c^2 = 0.4$), $\cdots\sigma^*\sigma'\pi^2\pi^{*2}$ ($c^2 = 0.25$), and $\cdots\sigma^*\sigma'\pi^3\pi^*$ ($c2 = 0.21$) constitute the $^5\Sigma^+$ state. The $2^5\Sigma^+$ state is also bound, and its spectroscopic parameters and composition are comparable with those of $^5\Sigma^+$. The computed energy separation between these two $^5\Sigma^+$ states is about 6632 cm^{-1}. Three closely spaced high-lying $^5\Pi$ states, which dissociate into higher asymptotes, are shown in Fig. 1a. The $3^5\Pi$ state is found to have a shallow potential well, while $2^5\Pi$ and $4^5\Pi$ states are more strongly bound with transition energies 34,801 and 40,755 cm^{-1}, respectively. The remaining $5^5\Pi$ and $^5\Delta$ states are lying above 40,000 cm^{-1}. The dominant configuration, which describes the $^5\Delta$ state, is found to be $\cdots\sigma^*\sigma'\pi^3\pi^*$.

3.2. Effects of the spin–orbit coupling and spectroscopic constants of Ω states

The introduction of the spin–orbit interaction in the Hamiltonian through spin–orbit operators results a number of Ω states which are discussed in this section. In the present calculations, 22 Λ–S states of InBi correlating with the lowest two dissociation limits are included in the spin–orbit CI treatment. Six asymptotes, which are correlated with 51 Ω states, are shown in Table 2. The calculated relative energies in various dissociation limits are compared with the experimental values. The $^2P_{3/2}$–$^2P_{1/2}$ energy splitting for the In atom, obtained from the MRDCI calculation of InBi at a very long bond length, is 2016 cm^{-1} which compares well with the observed value of 2213 cm^{-1}. The ($^2D_{3/2}$–$^2D_{5/2}$) splitting of Bi is overestimated in this calculation by about 700 cm^{-1}. However, relative energies of the dissociation limits from the ($^2P + {}^2D$) asymptote are found to be higher than the experimental values by 700–1600 cm^{-1}. At the same level of MRDCI treatment, other molecules in the group such as InP, InAs, and InSb show larger discrepancies.

Potential energy curves of low-lying 51 Ω states of 0^+, 0^-, 1, 2, 3, and 4 symmetries are plotted in Fig. 2a–d. All these Ω states arising out of 22 Λ–S states interact through the spin–orbit coupling which is considerably large for InBi compared with other InX (X = P, As, Sb) molecules. As a result of strong spin–orbit interactions, some of the potential energy curves change their shapes. Spectroscopic constants of a few low-lying bound Ω states of InBi are given in Table 3. The spin–orbit splitting of the ground state ($X^3\Sigma^-$) of InBi is estimated to be 761 cm^{-1}, with the $X_1 0^+$ component lying below the other ($X_2 1$). No experimental value of the zero-field splitting [$^3\Sigma^-(X_2 1)$–$^3\Sigma^-(X_1 0^+)$] for InBi has been reported so far. However, the zero-field splittings of InAs and InSb are 119 and 473.4 cm^{-1}, respectively, observed from the infrared spectra of molecules in rare-gas matrices. Table 4 shows the contributions of Λ–S states participated in the spin–orbit mixing at four representative bond distances. In the Franck–Condon region, $X_1 0^+$ is composed of two interacting components such as $X^3\Sigma^-_{0^+}$ and $^1\Sigma^+_{0^+}$, while the $X_2 1$ component is a strong mixture of $X^3\Sigma^-_1$, $^3\Pi_1$, and $^1\Pi_1$. In the shorter bond length region, the contributions of $^3\Pi$ in both $X_1 0^+$ and $X_2 1$ components become dominant. As a result, the equilibrium bond length of the adiabatic curve of

Table 3
Spectroscopic parameters of low-lying Ω states of InBi

State	T_e (cm^{-1})	r_e (Å)	ω_e (cm^{-1})
$X_1 0^+$	0	3.10	111
$X_2 1$	761	3.03	117
$^3\Pi_2$	1711	2.95	123
$^3\Pi_{0^+}$	5759	2.95	125
$^3\Pi_1$	8987	3.03	10^9
$^5\Pi_{0^+}$	9681	3.66	52
2(III)	13,721	3.06	110
$^1\Sigma^+_{0^+}$	15,541	2.91	143
0^-(III)	15,768	3.17	109
0^+(V)	19,681	3.42	66
0^+(VI)	22,113	3.51	78
$A0^+$	24,264	3.39	76

Table 4
Compositions of Ω states of InBi at four different bond lengths

State	Composition (in percentage contribution)			
	$r = 4.5$ a$_0$	$r = 5.0$ a$_0$	$r = r_e$	$r = 7.0$ a$_0$
$X_1 0^+$	$^3\Pi(43)$, $^1\Sigma^+(37)$, $X^3\Sigma^-(15)$	$X^3\Sigma^-(60)$, $^3\Pi(17)$, $^1\Sigma^+(13)$,$^5\Pi(4)$, $2^1\Sigma^+(3)$	$X^3\Sigma^-(73)$, $^1\Sigma^+(14)$, $^3\Pi(4)$, $^5\Pi(4)$	$X^3\Sigma^-(72)$, $^1\Sigma^+(15)$, $^5\Pi(5)$
$X_2 1$	$^3\Pi(54)$, $^1\Pi(25)$, $X^3\Sigma^-(17)$	$^3\Pi(40)$, $X^3\Sigma^-(34)$, $^1\Pi(20)$	$X^3\Sigma^-(52)$, $^3\Pi(26)$, $^1\Pi(13)$	$X^3\Sigma^-(59)$, $^3\Pi(13)$, $^1\Pi(9)$, $^5\Pi(7)$, $2^3\Pi(3)$
$^3\Pi_2$	$^3\Pi(90)$, $^1\Delta(7)$	$^3\Pi(84)$, $^1\Delta(12)$	$^3\Pi(77)$, $^1\Delta(17)$	$^3\Pi(64)$, $^1\Delta(16)$, $^5\Sigma^-(5)$, $3^1\Delta(4)$, $2^3\Pi(3)$
$^3\Pi_{0^+}$	$X^3\Sigma^-(57)$, $2^1\Sigma^+(24)$, $^3\Pi(8)$, $^1\Sigma^+(4)$,$^5\Pi(3)$	$^3\Pi(48)$, $2^1\Sigma^+(27)$, $X^3\Sigma^-(13)$, $^1\Sigma^+(6)$	$^3\Pi(64)$, $2^1\Sigma^+(26)$	$^3\Pi(67)$, $2^1\Sigma^+(10)$, $3^1\Sigma^+(7)$, $5^3\Pi(5)$, $4^3\Pi(4)$
$^3\Pi_1$	$^3\Pi(42)$, $^1\Pi(28)$, $X^3\Sigma^-(24)$	$X^3\Sigma^-(49)$, $^3\Pi(45)$, $^5\Pi(3)$	$^3\Pi(56)$, $X^3\Sigma^-(34)$, $^1\Pi(3)$, $^5\Pi(3)$	$^5\Pi(38)$, $^3\Pi(26)$, $2^3\Pi(8)$, $5^3\Pi(6)$, $4^1\Pi(5)$, $3^3\Delta(3)$
$^5\Pi_{0^+}$	$^1\Sigma^+(55)$, $^3\Pi(35)$, $2^1\Sigma^+(4)$	$^1\Sigma^+(69)$, $^3\Pi(12)$, $X^3\Sigma^-(8)$, $5^3\Pi(3)$	$^5\Pi(62)$, $5^3\Pi(9)$, $4^3\Sigma^-(8)$, $X^3\Sigma^-(5)$, $A^3\Pi(4)$, $2^1\Sigma^+(4)$	$^5\Pi(62)$, $4^3\Sigma^-(9)$, $5^3\Pi(8)$, $X^3\Sigma^-(5)$, $2^1\Sigma^+(5)$, $A^3\Pi(4)$
2(III)	$^5\Pi(59)$, $^3\Delta(17)$, $2^1\Delta(9)$, $^1\Delta(6)$, $5^3\Pi(4)$	$^5\Pi(65)$, $^3\Delta(6)$, $3^3\Delta(6)$, $2^1\Delta(5)$, $5^3\Pi(5)$, $^1\Delta(4)$	$^1\Delta(77)$, $^3\Pi(17)$	$2^3\Pi(36)$, $^5\Sigma^-(16)$, $3^1\Delta(10)$, $^1\Delta(8)$, $^3\Pi(6)$, $5^3\Pi(6)$, $^5\Pi(5)$, $6^3\Pi(4)$
$^1\Sigma^+_{0^+}$	$^5\Pi(70)$, $2^3\Pi(10)$, $5^3\Pi(9)$, $X^3\Sigma^-(4)$	$^5\Pi(65)$, $2^3\Pi(10)$, $5^3\Pi(8)$, $^1\Sigma^+(8)$	$^1\Sigma^+(78)$, $^5\Pi(8)$, $X^3\Sigma^-(5)$, $^3\Pi(3)$	$^1\Sigma^+(41)$, $2^3\Pi(38)$, $X^3\Sigma^-(7)$, $4^3\Pi(6)$
0^-(III)	$^3\Sigma^+(52)$, $2^3\Pi(23)$, $A^3\Pi(9)$, $^1\Sigma^-(9)$, $^5\Pi(3)$	$2^3\Pi(43)$, $^3\Sigma^+(33)$, $^5\Pi(8)$, $^1\Sigma^-(6)$, $2^1\Sigma^-(5)$, $A^3\Pi(4)$	$2^3\Pi(47)$, $^3\Pi(19)$, $^3\Sigma^+(12)$, $2^1\Sigma^-(9)$, $4^3\Pi(4)$, $2^3\Sigma^+(4)$	$^5\Sigma^-(76)$, $3^3\Sigma^+(12)$, $6^3\Pi(8)$
0^+(V)	$2^3\Pi(53)$, $2^1\Sigma^+(20)$, $A^3\Pi(11)$, $^5\Pi(9)$	$2^3\Pi(58)$, $^5\Pi(18)$, $A^3\Pi(12)$, $2^1\Sigma^+(7)$, $5^3\Pi(3)$	$2^3\Pi(32)$, $^5\Pi(24)$, $A^3\Pi(16)$, $2^1\Sigma^+(8)$, $3^1\Sigma^+(7)$, $2^3\Sigma^-(6)$, $5^3\Pi(3)$	$^5\Pi(24)$, $A^3\Pi(20)$, $2^3\Pi(13)$, $2^3\Sigma^-(11)$, $2^1\Sigma^+(10)$, $^1\Sigma^+(8)$, $3^1\Sigma^+(6)$, $5^3\Pi(4)$
0^+(VI)	$2^1\Sigma^+(34)$, $2^3\Pi(18)$, $X^3\Sigma^-(12)$, $^3\Pi(9)$, $A^3\Pi(6)$, $^5\Pi(6)$, $4^3\Pi(5)$, $5^3\Pi(5)$	$2^1\Sigma^+(52)$, $^3\Pi(18)$, $X^3\Sigma^-(14)$, $5^3\Pi(6)$, $2^3\Sigma^-(3)$	$2^3\Pi(34)$, $2^3\Sigma^-(21)$, $4^3\Pi(12)$, $A^3\Pi(10)$, $2^1\Sigma^+(8)$, $3^1\Sigma^+(4)$	$2^3\Pi(27)$, $4^3\Pi(21)$, $2^3\Sigma^-(14)$, $^3\Pi(9)$, $2^1\Sigma^+(8)$, $3^3\Sigma^-(6)$, $3^1\Sigma^+(5)$, $A^3\Pi(3)$, $^1\Sigma^+(3)$
$A0^+$	$A^3\Pi(39)$, $3^1\Sigma^+(19)$, $2^3\Sigma^-(18)$, $5^3\Pi(9)$, $2^3\Pi(4)$, $2^1\Sigma^+(4)$, $X^3\Sigma^-(3)$	$A^3\Pi(80)$, $2^3\Pi(13)$	$A^3\Pi(46)$, $2^3\Sigma^-(13)$, $4^3\Pi(10)$, $^1\Sigma^+(8)$, $3^1\Sigma^+(7)$, $^3\Pi(7)$, $3^3\Sigma^-(3)$	$A^3\Pi(57)$, $^1\Sigma^+(12)$, $2^3\Sigma^-(7)$, $3^1\Sigma^+(4)$, $2^1\Sigma^+(3)$, $^3\Pi(3)$, $2^1\Sigma^+(3)$, $^3\Pi(3)$, $2^3\Pi(3)$, $3^3\Sigma^-(3)$, $4^3\Sigma^-(3)$

$X_2 1$ becomes shorter and vibrational frequency larger than the $X_1 0^+$ component.

Four components of the first excited state ($^3\Pi$) split as 2, 0^+, 1, and 0^- in the increasing order of energy. The effect of the spin–orbit coupling on this state is considerably large. The $^3\Pi_{0^-}$ component is shifted up to a large extent. In addition, there is an avoided crossing with the $^5\Pi_{0^-}$ curve which makes the potential minimum of the $^3\Pi_{0^-}$ state to disappear (Fig. 2b). The component with $\Omega = 2$ becomes the most stable of all four components of $^3\Pi$ with $T_e = 1711\ \text{cm}^{-1}$ and $r_e = 2.95$ Å. As seen in Table 4, the dominant $^3\Pi_2$ component interacts strongly with $^1\Delta_2$ throughout the potential curve. In the longer bond length region, other $\Omega = 2$ components, namely, $^5\Sigma_2^-$, $^3\Delta_2$, $2^3\Pi_2$, etc. contribute to a small extent. In general, adiabatic curves are fitted for estimating the spectroscopic constants. The potential minimum of $^3\Pi_{0^+}$ lies $5759\ \text{cm}^{-1}$ above the ground state with $r_e = 2.95$ Å and $\omega_e = 125\ \text{cm}^{-1}$. The spin–orbit CI wave functions show that the mixing of $^3\Pi_{0^+}$ with the $2^1\Sigma_{0^+}^+$ component is considerably large. In the shorter bond length region, an avoided crossing with the $X^3\Sigma_{0^+}^-$ component takes place. The $^3\Pi_1$ state is found to be weakly bound. Although dominated by the component of $^3\Pi$, a strong coupling with $X^3\Sigma_1^-$ shifts the bond length of the $^3\Pi_1$ state to a longer value ($r_e = 3.03$ Å). The estimated transition energy of the fitted adiabatic curve of the $^3\Pi_1$ state is about $8987\ \text{cm}^{-1}$. The compositions of the state at different bond lengths are shown in Table 4.

Third 0^+ state, designated as $^5\Pi_{0^+}$ shows a very shallow potential minimum at $r = 3.66$ Å. Although the $^5\Pi$ state is repulsive, a minimum appears in the curve of $^5\Pi_{0^+}$ due to strong coupling with the neighbouring components. No other spin–orbit components of $^5\Pi$ show any bound character. The fitted adiabatic potential curve of the fourth root of the 0^+ symmetry gives an estimate of $r_e = 2.91$ Å and $\omega_e = 143\ \text{cm}^{-1}$. In the bond length region below 5.2 a_0, the curve is dominated by the $^5\Pi_{0^+}$ component, while in the equilibrium and longer bond region, it is mainly described by the 0^+ component of $^1\Sigma^+$. Thus the state is designated as $^1\Sigma_{0^+}^+$. The spin–orbit coupling has pushed up the only component of $^1\Sigma^+$ to a large extent, and the estimated T_e of $^1\Sigma_{0^+}^+$ is $15{,}541\ \text{cm}^{-1}$ as compared with $9105\ \text{cm}^{-1}$ of $^1\Sigma^+$. Next three roots of $\Omega = 0^+$ have shallow potential minima. The 0^+(V) curve in Fig. 2a has a minimum at 3.42 Å. The spin–orbit CI wave functions show that the 0^+(V) state is composed of many Λ–S states with different contributions at different bond lengths (Table 4). The maximum contribution to the 0^+(V) state in the Franck–Condon region comes from $2^3\Pi$. In the bond length region above 7.0 a_0, the contribution of the $2^3\Pi_{0^+}$ component diminishes. The estimated transition energy of 0^+(V) is nearly $5000\ \text{cm}^{-1}$ above that of $2^3\Pi$. The next two 0^+ states, which are denoted as 0^+(VI) and $A0^+$, are both weakly bound, with transition energies 22,113 and $24{,}264\ \text{cm}^{-1}$, respectively. The $A0^+$ state has a comparatively shorter bond length ($r_e = 3.39$ Å) and it is bound by about $1300\ \text{cm}^{-1}$. The present calculations suggest that the 0^+(VI) state is a result of a strong coupling among the $\Omega = 0^+$ components of many states such as $2^1\Sigma^+$, $2^3\Pi$, $A^3\Pi$, $2^3\Sigma^-$, $^3\Pi$, etc. while in $A0^+$, the largest contribution comes from the $A^3\Pi_{0^+}$ component. Similar with other group III–V diatomic molecules, $\Omega = 0^+$ is the only component of $A^3\Pi$, which survives any predissociation. Other components of $A^3\Pi$ undergo predissociations mainly due to strong interaction with the corresponding spin–orbit components of the repulsive $^5\Sigma^-$ state. Transitions from any of these excited 0^+ states to the ground-state component ($X0^+$) are expected to be quite strong. In this regard, the $A0^+$–$X0^+$ transition may be compared with $A^3\Pi_{0^+}$–$X^3\Sigma_{0^+}^-$ of all isovalent group III–V diatomic molecules. In the subsequent section, the $A0^+$–$X0^+$ transition probabilities are discussed in detail. The potential energy curve of 2(III) shows two avoided crossings (Fig. 2c). The first one is between $^5\Pi_2$ and $^1\Delta_2$ near 5.5 a_0, while the second is between $^1\Delta_2$ and $\Omega = 2$ components of many states such as $2^3\Pi$, $^5\Sigma^-$, etc. The potential minimum of the adiabatic 2(III) curve is obtained at 3.06 Å with $\omega_e = 110\ \text{cm}^{-1}$. The potential well of the 2(III) state consists of only 2–3 vibrational nodes. There exists a couple of shallow minima in the high-energy curves of states of $\Omega = 2$ symmetry. However, these are not significant from the spectroscopic point of view. The adiabatic curve of the third root of 0^- shows a minimum at 3.17 Å with $\omega_e = 109\ \text{cm}^{-1}$. The potential well of 0^-(III) has been found to hold six vibrational nodes and the state is expected to dissociate through the channel dominated by the repulsive curve of the $^5\Sigma^-$ symmetry (Fig. 2b).

The apparent double minimum in the potential curve of the sixth root of $\Omega = 1$ is due to several avoided crossings involving the components such as $A^3\Pi_1$, $2^3\Pi_1$, $^1\Pi_1$, $^5\Sigma_1^-$, $X^3\Sigma_1^-$, etc. This has been confirmed from the analysis of wave functions at various bond lengths as shown in Table 4.

3.3. Transition moments and radiative lifetimes of excited states

In order to identify possible dipole-allowed transitions, transition dipole moments are estimated in the present MRDCI calculations of InBi. At the Λ–S level, two singlet–singlet and two triplet–triplet transitions are found to be probable. In Fig. 3a, we have plotted transition moments of these transitions, namely, $2^1\Sigma^+ - ^1\Sigma^+$, $2^1\Sigma^+ - ^1\Pi$, $A^3\Pi - X^3\Sigma^-$, and $A^3\Pi - ^3\Pi$ as a function of the internuclear distance. Table 5 shows the radiative lifetimes of excited states at the lowest three vibrational levels. The transition-moment curve of the A–X transition shows a maximum. The transition-moment values of $A^3\Pi - X^3\Sigma^-$ and $2^1\Sigma^+ - ^1\Pi$ transitions are comparable throughout the curves, and these transitions are expected to be strong. On the other hand, transition moments of $A^3\Pi - ^3\Pi$ are comparatively small in the Franck–Condon region of the curve. The radiative partial lifetime of $A^3\Pi$ at $v' = 0$ computed from the transition probability of $A^3\Pi - X^3\Sigma^-$ has been found to be 1.03 μs, while the same obtained from $A^3\Pi - ^3\Pi$ is about 4.2 ms. Summing up the transition probabilities of these two transitions, the total lifetime of $A^3\Pi$ at $v' = 0$ becomes 1.0 μs. As seen in Fig. 3a, the transition moment of $2^1\Sigma^+ - ^1\Sigma^+$ increases upto $r = 5.3$ a_0 and then drops quickly at larger internuclear distances. The present calculations predict the $2^1\Sigma^+ - ^1\Pi$ transition to be stronger than $2^1\Sigma^+ - ^1\Sigma^+$. The estimated total lifetime of the $2^1\Sigma^+$ state at the lowest vibrational level is about 7.2 μs.

The dipole moments of three electronic states, namely, $X^3\Sigma^-$, $^3\Pi$, and $A^3\Pi$ of InBi are also plotted in Fig. 3a as a function of the bond length. The ground-state dipole moment decreases monotonically with r, while the dipole curve of the $^3\Pi$ state shows a minimum around 6.25 a_0 due to an avoided crossing

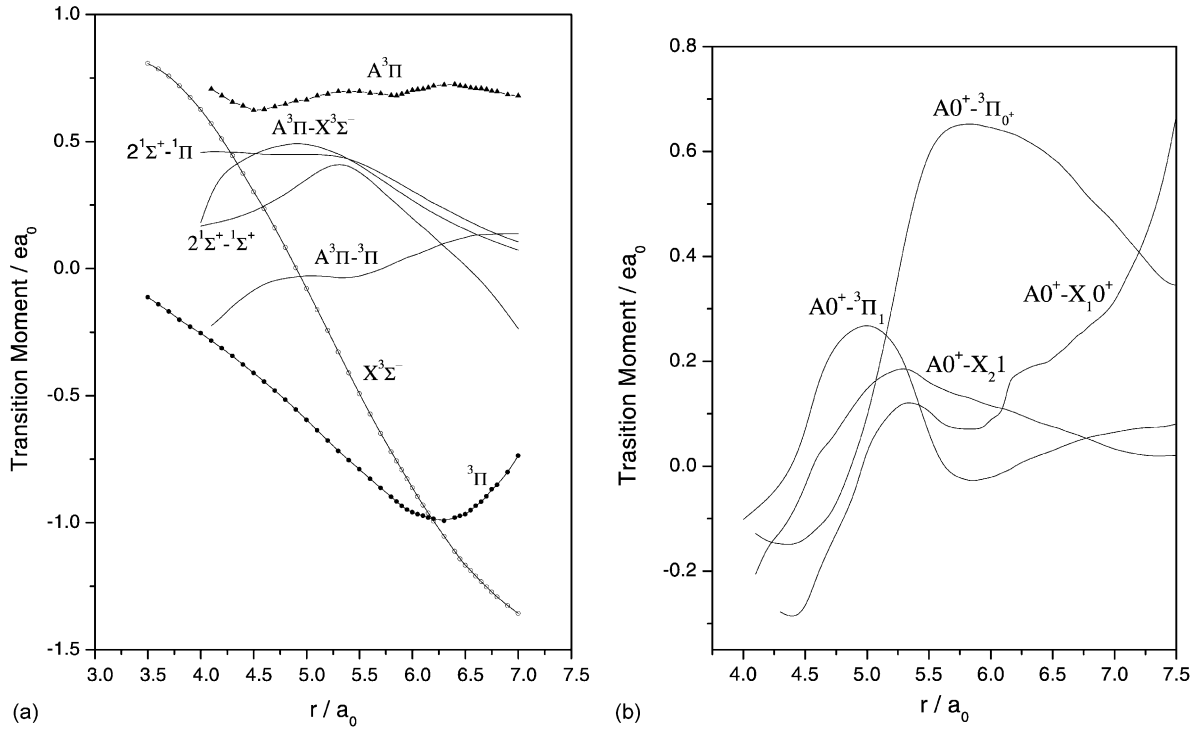

Fig. 3. (a) Transition-moment functions of four transitions involving Λ–S states, and dipole moment functions of $X^3\Sigma^-$ (open circle), $^3\Pi$ (filled circle) and $A^3\Pi$ (up triangle) states of InBi. (b) Transition-moment functions of transitions from the $A0^+$ component of InBi.

Table 5
Radiative lifetimes(s) of some excited states at few lowest vibrational levels of InBi

Transition	Lifetime of the upper state			Total lifetime of the upper state at $v' = 0$
	$v' = 0$	$v' = 1$	$v' = 2$	
$A^3\Pi - X^3\Sigma^-$	1.03(−6)	1.05(−6)	1.07(−6)	
$A^3\Pi - {}^3\Pi$	0.42(−4)	0.35(−4)	0.31(−4)	$\tau(A^3\Pi) = 1.0(-6)$
$2^1\Sigma^+ - {}^1\Pi$	9.42(−6)	9.40(−6)	9.39(−6)	
$2^1\Sigma^+ - {}^1\Sigma^+$	3.04(−5)	3.04(−5)	3.04(−5)	$\tau(2^1\Sigma^+) = 7.2(-6)$
$A0^+ - X_1 0^+$	1.15(−6)	1.25(−6)	1.24(−6)	
$A0^+ - X_2 1$	4.33(−6)	4.33(−6)	4.45(−6)	
$A0^+ - {}^3\Pi_{0^+}$	0.25(−6)	0.27(−6)	0.27(−6)	$\tau(A0^+) = 0.20(-6)$

Values in parentheses are the powers to the base 10.

with $2^3\Pi$ as shown in their potential energy curves. As noted before, the $\sigma'\pi^2\pi^*$ configuration of the $^3\Pi$ state starts mixing strongly with another important configuration, namely, $\sigma'\pi^3$ in the longer bond length region. Since π is a nonbonding MO localized on Bi and π^* is antibonding with its charge center away from the Bi atom, the dipole-moment curve of the $^3\Pi$ state shows a minimum in the longer bond length region. The dipole moment of InBi in the $A^3\Pi$ state does not change much with the bond length. The computed dipole moment values of $X^3\Sigma^-$, $^3\Pi$ and $A^3\Pi$ at r_e of the ground state are -0.761, -0.915, and 0.688 ea_0, respectively. It may be mentioned that the negative value corresponds to the In^+Bi^- polarity. No experimental dipole moment of InBi has been reported so far.

Unlike other group III–V molecules, the $A^3\Pi_{0^+}$ component of InBi is heavily mixed up. We have considered four transitions arising out of $A0^+$. These are $A0^+ - X_1 0^+$, $A0^+ - X_2 1$, $A0^+ - {}^3\Pi_{0^+}$, and $A0^+ - {}^3\Pi_1$ whose transition moments are plotted in Fig. 3b as function of r. It may be mentioned here that all dipole and transition moments vanish at a very large bond length ($r > 10\ a_0$). The computed transition moments of $A0^+ - {}^3\Pi_{0^+}$ is much larger than those of other transitions. The estimated partial lifetime of $A0^+$ at $v' = 0$ is about 0.25 μs which suggests that the $A0^+ - {}^3\Pi_{0^+}$ transition is highly probable around 24,000 cm^{-1}. The transition of $A0^+$ to the $^3\Pi_1$ state is predicted to be weak because of the negligible Franck–Condon factor. Transition moments of $A0^+ - X_1 0^+$ and $A0^+ - X_2 1$ are found to be comparable in the Franck–Condon region. The calculated partial lifetimes of $A0^+$ for both transitions are of the order of microseconds. Table 5 displays these lifetimes at three lowest vibrational levels. After adding three transition probabilities, the total lifetime of $A0^+$ is calculated to be about 0.2 μs.

3.4. Comparison of the electronic spectrum of InX (X = P, As, Sb, Bi) molecules

Ab initio based MRDCI calculations of InP, InAs, and InSb have been reported in recent years [36,37,39]. Although the detail experimental results are lacking, the computed electronic structure and spectroscopic features of these molecules in the low-lying states are made available. It is, therefore, appropriate to compare those results with the spectroscopic aspects of the InBi molecule obtained in the present study. Table 6 displays the summary of the computed spectroscopic properties of all four InX molecules. In the absence of any spin–orbit coupling, the ground states ($X^3\Sigma^-$) of all four indium molecules have $\cdots\sigma^2\sigma^{*2}\sigma'^2\pi^2$ as the dominating configuration. The equilibrium bond length, vibrational frequency, and dissociation energy of the ground-state molecules follow the expected trend. The r_e value increases while ω_e and D_e decrease from InP to InBi. The experimental D_0^0 values, wherever available, are found to be higher than the computed values by about 0.2–0.5 eV. The dipole moments of the ground-state InX molecules do not change much with the mass of the molecule. The bond lengths of the first excited state ($^3\Pi$) of all four molecules are consistently shorter than those of the ground-state bond due to the $\sigma' \rightarrow \pi$ excitation which increases the delocalization through the occupancy of π MO. The $\Delta E(^1\Pi - {}^3\Pi)$ energy

Table 6
Comparison of spectroscopic features of InX (X = P, As, Sb, Bi) molecules computed at the same level of MRDCI treatment

Property[a]	InP[b]	InAs[c]	InSb[d]	InBi
$r_e(X^3\Sigma^-)$ (Å)	2.71	2.76	3.02	3.10
$\omega_e(X^3\Sigma^-)$ (cm^{-1})	248	179	139	120
$D_e(X^3\Sigma^-)$ (eV)	1.48	1.31	1.22	1.16
$\mu_e(X^3\Sigma^-)$ (D)	1.86	1.85	2.16	1.93
$T_e(^3\Pi)$ (cm^{-1})	2288	1916	2654	2893
$r_e(^3\Pi)$ (Å)	2.51	2.56	2.81	2.88
$\Delta E(^1\Pi-^3\Pi)$ (cm^{-1})	4665	4608	4351	4290
$T_e(A^3\Pi)$ (cm^{-1})	22,082	21,076	20,108	19,365
$r_e(A^3\Pi)$ (Å)	2.75	2.79	3.07	3.18
$\omega_e(A^3\Pi)$ (cm^{-1})	219	163	111	88
zfs (cm^{-1})[e]	40	92	429	761
$T_e(A^3\Pi_{0^+})$ (cm^{-1})	21,675	20,918	20,094	24,264
$r_e(A^3\Pi_{0^+})$ (Å)	2.79	2.85	3.16	3.39
$\omega_e(A^3\Pi_{0^+})$ (cm^{-1})	227	148	102	76
$\tau_{A^3\Pi}$, (μs)	0.19	0.25	0.53	1.00
$\tau_{A^3\Pi_{0^+}}$, (μs)	0.456	0.436	2.50	0.20

[a] The subscript e refers to the parameter at r_e of the corresponding state.
[b] Ref. [37].
[c] Ref. [39].
[d] Ref. [36].
[e] Zero field splitting [$^3\Sigma^-(X_21)-^3\Sigma^-(X_10^+)$].

splittings of InP and InAs are comparable in magnitude, while the smallest splitting of 4290 cm^{-1} is predicted for InBi.

For diatomic molecules of group III and V, the A–X transition is well known. The A state is generally found to be the third root of the $^3\Pi$ symmetry. Although the A–X transition is not observed experimentally for any of the InX molecules, the MRDCI calculations predict strong $A^3\Pi-X^3\Sigma^-$ transitions for all four molecules in the range 19,000–22,000 cm^{-1}. The smallest transition energy is obtained for the heavier molecule InBi. Table 6 shows that the radiative lifetime of the $A^3\Pi$ state increases steadily from InP to InBi. The lighter molecule InP has the shortest lifetime of 0.19 μs in the $A^3\Pi$ state. As expected, effects of the spin–orbit coupling on the electronic states are largest for InBi. Many avoided curve crossings change the spectroscopic properties and potential energy curves of InBi to a larger extent compared to those of InP, InAs, and InSb. It is exemplified in Table 6 where the zero-field splitting of the ground state ($X^3\Sigma^-$) of InBi is found to be the largest (~761 cm^{-1}) of all four molecules compared. Such splittings for InP and InAs are negligibly small. For the lighter molecules such as InP, InAs, and InSb, the $\Omega = 0^+$ component of $A^3\Pi$ remains almost pure and it has been found that $A^3\Pi_{0^+}$ survives predissociation and forms bound state from which transitions to low-lying 0^+ and 1 components become probable. The remaining components 0^-, 1, and 2 of $A^3\Pi$ are found to undergo predissociations through interactions with suitable components of the repulsive $^5\Sigma^-$ state. Because of the strongest spin–orbit mixing in InBi, the $A^3\Pi_{0^+}$ component consists of many other states, and it is denoted here as $A0^+$. The transition energy of the $A0^+$ component of InBi at equilibrium is the largest of all due to the strongest spin–orbit coupling. The computed lifetime of the surviving component $A^3\Pi_{0^+}$ changes its trend from InP to InBi. The $A0^+$ state of InBi is found to be shortest-lived.

4. Concluding remarks

Ab initio based MRDCI calculations using RECP and Gaussian basis sets, which include diffused functions, predict a fairly accurate picture of the electronic spectrum of the InBi molecule. There are at least 20 Λ–S states which have bound potential

energy curves within 40,000 cm^{-1}. The r_e and ω_e of the ground state ($X^3\Sigma^-$) of InBi are predicted to be 3.1 Å and 120 cm^{-1}, respectively. Although no experimental results are available for this molecule, the present method is known to overestimate r_e and underestimate ω_e because of the use of RECP and the absence of d-correlation. Several quintet bound states are noted above 28,000 cm^{-1} of energy. The computed dissociation energy of the ground state of InBi is 114 kJ mol^{-1} which is smaller than the experimental value by about 39 kJ mol^{-1}. It has been found that the d-correlation in CI does not change the ground-state dissociation energy of InBi much. But the r_e of the ground state is improved by about 0.04 Å, while the ω_e value is increased only by 7 cm^{-1}. The dissociation energies show correct trend when compared with D_e values of other members in the group. The transition energy of $A^3\Pi$ of InBi is found to be lowest among InX (X = P, As, Sb, Bi) molecules. The spin–orbit coupling is found to be strongest in InBi. The calculated zero-field splitting of the ground-state InBi is 761 cm^{-1}, which is considerably large compared with other InX molecules. The $X_1 0^+$ component is lying lower than $X_2 1$. All Ω states of InBi show strong spin–orbit interaction, and they do not remain as pure Λ–S character. Many avoided curve crossings result predissociations. The $A0^+$ state of InBi survives the predissociation and is expected to undergo strong transitions to the ground-state components $X_1 0^+$ and $X_2 1$ in the range 23,500–24,500 cm^{-1}. Other components originating from $A^3\Pi$ predissociate. At the lowest vibrational level ($v' = 0$), the radiative lifetime of $A0^+$ estimated from the spin–orbit CI wave functions is found to be 0.2 μs.

Acknowledgements

We thank Prof. Dr Robert J. Buenker, Wuppertal, Germany, for his kind permission to use his CI codes for the present calculations.

References

[1] S.C. O'Brien, Y. Liu, Q. Zhang, J.R. Heath, F.K. Tittel, R.F. Curl, R.E. Smalley, J. Chem. Phys. 84 (1986) 4074.
[2] Y. Liu, Q. Zhang, F.K. Tittel, R.F. Curl, R.E. Smalley, J. Chem. Phys. 85 (1986) 7434.
[3] Q. Zhang, Y. Liu, R.F. Curl, F.K. Tittel, R.E. Smalley, J. Chem. Phys. 88 (1988) 1670.
[4] L. Wang, L.P.F. Chibante, F.K. Tittel, R.F. Curl, R.E. Smalley, Chem. Phys. Lett. 172 (1990) 335.
[5] C. Jin, K. Taylor, J. Conciecao, R.E. Smalley, Chem. Phys. Lett. 175 (1990) 17.
[6] L. Lou, L. Wang, L.P.F. Chibante, R.T. Laaksonen, P. Nordlanden, R.E. Smalley, J. Chem. Phys. 94 (1991) 8015.
[7] G.W. Lemire, G.A. Bishea, S.A. Heidecke, M.D. Morse, J. Chem. Phys. 92 (1990) 121.
[8] C.C. Arnold, D.M. Neumark, J. Chem. Phys. 99 (1994) 3353.
[9] C.C. Arnold, D.M. Neumark, J. Chem. Phys. 100 (1994) 1797.
[10] C. Xu, E. deBeer, D.W. Arnold, C.C. Arnold, D.M. Neumark, J. Chem. Phys. 101 (1994) 5406.
[11] C.C. Arnold, D.M. Neumark, Can. J. Phys. 72 (1994) 1322.
[12] G.R. Burton, C. Xu, C.C. Arnold, D.M. Neumark, J. Chem. Phys. 104 (1996) 2757.
[13] S. Li, R.J. Van Zee, W. Weltner Jr., J. Phys. Chem. 97 (1993) 11393.
[14] R.J. Van Zee, S. Li, W. Weltner Jr., J. Chem. Phys. 98 (1993) 4335.
[15] S. Li, R.J. Van Zee, W. Weltner Jr., J. Phys. Chem. 98 (1994) 2275.
[16] S. Li, R.J. Van Zee, W. Weltner Jr., J. Chem. Phys. 100 (1994) 7079.
[17] V. Piacente, A. Desideri, J. Chem. Phys. 57 (1972) 2213.
[18] G. Riekert, G. Rainer-Harbach, P. Lamparter, S. Steeb, Z. Metallkd. 76 (1981) 406.
[19] K. Balasubramanian, Relativistic Effects in Chemistry Part A. Theory and Techniques, Wiley-Intersciences, New York, 1997.
[20] K. Balasubramanian, Relativistic Effects in Chemistry Part B. Applications to Molecules and Clusters, Wiley-Intersciences, New York, 1997.
[21] (a) K. Balasubramanian, J. Chem. Phys. 86 (1987) 3410.
(b) Erratum.K. Balasubramanian, J. Chem. Phys. 92 (1990) 2123.
[22] K. Balasubramanian, J. Mol. Spectrosc. 139 (1990) 405.
[23] K. Balasubramanian, Chem. Rev. 90 (1990) 93.
[24] K. Balasubramanian, J. Chem. Phys. 93 (1990) 507.
[25] K.K. Das, K. Balasubramanian, J. Chem. Phys. 94 (1991) 6620.
[26] P.Y. Feng, K. Balasubramanian, Chem. Phys. Lett. 265 (1997) 41.
[27] P.Y. Feng, K. Balasubramanian, Chem. Phys. Lett. 265 (1997) 547.
[28] P.Y. Feng, K. Balasubramanian, Chem. Phys. Lett. 283 (1998) 167.
[29] P.Y. Feng, K. Balasubramanian, Chem. Phys. Lett. 284 (1998) 313.
[30] U. Meier, S.D. Peyerimhoff, P.J. Bruna, F. Grein, J. Mol. Spectroc. 134 (1989) 259.

[31] V. Musolino, M. Toscano, N. Russo, J. Comput. Chem. 11 (1990) 924.
[32] T. Oranges, V. Musolino, M. Toscano, N. Russo, Z. Phys. D-At. Mol. Clusters 17 (1990) 133.
[33] M. Toscano, N. Russo, Z. Phys. D-At. Mol. Clusters 22 (1992) 683.
[34] B. Manna, K.K. Das, J. Phys. Chem. A102 (1998) 9876.
[35] B. Manna, K.K. Das, J. Mol. Struct. (Theochem) 467 (1999) 135.
[36] B. Manna, A. Dutta, K.K. Das, J. Mol. Struct. (Theochem) 497 (2000) 123.
[37] B. Manna, A. Dutta, K.K. Das, J. Phys. Chem. A104 (2000) 2764.
[38] A. Dutta, A. Chattopadhyay, K.K. Das, J. Phys. Chem. A104 (2000) 9777.
[39] A. Dutta, D. Giri, K.K. Das, J. Phys. Chem. A105 (2001) 9049.
[40] A. Chattopadhyay, S. Chattopadhyaya, K.K. Das, J. Phys. Chem. A106 (2002) 2685.
[41] L.A. La John, P.A. Christiansen, R.B. Ross, T. Atashroo, W.C. Ermler, J. Chem. Phys. 87 (1987) 2812.
[42] S.A. Wildman, G.A. Dilabio, P.A. Christiansen, J. Chem. Phys. 107 (1997) 9975.
[43] R.J. Buenker, S.D. Peyerimhoff, Theor. Chim. Acta 35 (1974) 33.
[44] R.J. Buenker, S.D. Peyerimhoff, Theor. Chim. Acta 39 (1975) 217.
[45] R.J. Buenker, S.D. Peyerimhoff, W. Butcher, Mol. Phys. 35 (1978) 771.
[46] R.J. Buenker, in: P. Burton (Ed.), Proceedings of the Workshop on Quantum Chemistry and Molecular Physics, University Wollongong, Wollongong, 1980.
[47] R.J. Buenker, in: R. Carbó (Ed.), Studies in Physical and Theoretical Chemistry, Current Aspects of Quantum Chemistry, vol. 21, Elsevier, Amsterdam, 1981.
[48] R.J. Buenker, R.A. Phillips, J. Mol. Struct. (Theochem) 123 (1985) 291.
[49] R.J. Buenker, Int. J. Quantum Chem. 29 (1986) 435.
[50] E.R. Davidson, in: R. Daudel, B. Pullman (Eds.), The World of Quantum Chemistry, Reidel, Dordrecht, 1974.
[51] G. Hirsch, P.J. Bruna, S.D. Peyerimhoff, R.J. Buenker, Chem. Phys. Lett. 52 (1977) 442.
[52] J.W. Cooley, Math. Comput. 15 (1961) 363.
[53] C.E. Moore, Atomic Energy Levels, vol 3, National Bureau of Standards, Washington, DC.